

Hydrophobic Nature of the Active Site of Mandelate Racemase[†]

Martin St. Maurice and Stephen L. Bearne*

Department of Biochemistry and Molecular Biology, Dalhousie University, Halifax, Nova Scotia B3H 1X5, Canada

Received December 8, 2003

ABSTRACT: Mandelate racemase (EC 5.1.2.2) from *Pseudomonas putida* catalyzes the interconversion of the two enantiomers of mandelic acid with remarkable proficiency, stabilizing the altered substrate in the transition state by approximately 26 kcal/mol. We have used a series of substrate analogues (glycolates) and intermediate analogues (hydroxamates) to evaluate the contribution of the hydrophobic cavity within the enzyme's active site to ligand binding. Free energy changes accompanying binding of glycolate derivatives correlated well with the hydrophobic substituent constant π and the van der Waals surface areas of the ligands. The observed dependence of the apparent binding free energy on surface area of the ligand was $-30 \pm 5 \text{ cal mol}^{-1} \text{ \AA}^{-2}$ at 25 °C. Free energy changes accompanying binding of hydroxamate derivatives also correlated well with π values and the van der Waals surface areas of the ligands, giving a slightly greater free energy dependence equal to $-41 \pm 3 \text{ cal mol}^{-1} \text{ \AA}^{-2}$ at 25 °C. Surprisingly, mandelate racemase exhibited a binding affinity for the intermediate analogue benzohydroxamate that was 2 orders of magnitude greater than that predicted solely on the basis of hydrophobic interactions. This suggests that there are additional specific interactions that stabilize the altered substrate in the transition state. Mandelate racemase was competitively inhibited by (*R,S*)-1-naphthylglycolate (apparent $K_i = 1.9 \pm 0.1 \text{ mM}$) and (*R,S*)-2-naphthylglycolate (apparent $K_i = 0.52 \pm 0.03 \text{ mM}$), demonstrating the plasticity of the hydrophobic pocket. Both (*R*)- ($K_m = 0.46 \pm 0.06 \text{ mM}$, $k_{\text{cat}} = 33 \pm 1 \text{ s}^{-1}$) and (*S*)-2-naphthylglycolate ($K_m = 0.41 \pm 0.03 \text{ mM}$, $k_{\text{cat}} = 25 \pm 1 \text{ s}^{-1}$) were shown to be alternative substrates for mandelate racemase. These kinetic results demonstrate that no major steric restrictions are imposed on the binding of this bulkier substrate in the ground state but that steric factors appear to impair transition state/intermediate stabilization. 2-Naphthohydroxamate was identified as a competitive inhibitor of mandelate racemase, binding with an affinity ($K_i = 57 \pm 18 \text{ }\mu\text{M}$) that was reduced relative to that observed for benzohydroxamate and that was in accord with the ~ 10 -fold reduction in the value of k_{cat}/K_m for the racemization of 2-naphthylglycolate. These findings indicate that, for mandelate racemase, steric constraints within the hydrophobic cavity of the enzyme–intermediate complex are more stringent than those in the enzyme–substrate complex.

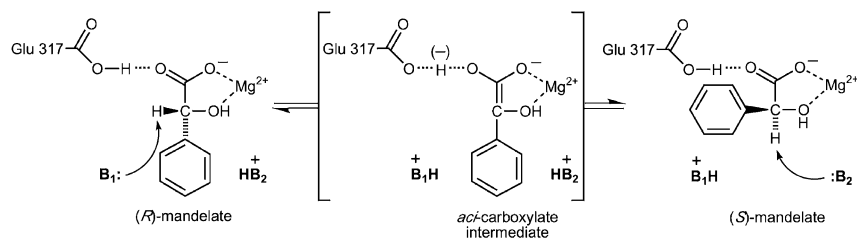
Mandelate racemase (MR;¹ EC 5.1.2.2) from *Pseudomonas putida* catalyzes the Mg^{2+} -dependent 1,1-proton transfer reaction that interconverts the enantiomers of mandelic acid (Scheme 1) (1–3). Isotope exchange, site-directed mutagenesis, and X-ray crystallographic experiments indicate that catalysis proceeds via a two-base mechanism, with His 297 and Lys 166 abstracting the α -proton from (*R*)-mandelate and (*S*)-mandelate, respectively (4–6). In addition, site-directed mutagenesis experiments have revealed that Glu 317 acts as a general acid catalyst (7) and Asn 197 interacts with the α -hydroxyl of mandelate to facilitate stabilization of the altered substrate in the transition state (8). The ability of MR to catalyze rapid carbon–hydrogen bond cleavage from a carbon acid with a relatively high $\text{p}K_a$ (9–11) makes it a useful paradigm for understanding enzyme-catalyzed proton abstraction from carbon acids (12–15).

Crystal structures of MR complexed with substrate and substrate analogues (5–7, 16) reveal the aromatic ring of all ground-state ligands located within a large hydrophobic cavity at the mouth of the enzyme active site, remote from the site of proton abstraction (Figure 1) (17). The cavity is composed of hydrophobic amino acid residues from both the N-terminal and central β -barrel domains of the enzyme and also includes Leu 93 from an adjacent 2-fold related subunit (17). A major component of the hydrophobic cavity is a large, mobile, amphipathic β -meander flap that extends over the active site (17). The hydrophobic cavity appears to accommodate a variety of substrates, including several para-substituted mandelic acids (18–20), *p*-(bromomethyl)mandelate (21), propargylglycolate (22), vinylglycolate (23), *o*-chloromandelate, and furyl-, thienyl-, and naphthyl-substituted glycolic acids (18). The wide spectrum of aryl- and heteroaryl-substituted mandelate derivatives that serve as substrates for MR suggests a relatively low degree of steric hindrance for substrate binding within the hydrophobic cavity. Despite this broad substrate specificity, β,γ -unsaturation is required for catalysis (23). For example, vinylglycolate is a substrate for MR while ethylglycolate is not (23). Hence, stabilization of the enolic/ate intermediate and/

[†] This work was supported by the Natural Sciences and Engineering Research Council of Canada (NSERC). M.St.M. is the recipient of an NSERC postgraduate scholarship.

* To whom correspondence should be addressed. Phone: (902) 494-1974. Fax: (902) 494-1355. E-mail: sbearne@dal.ca.

¹ Abbreviations: CD, circular dichroism; HEPES, 4-(2-hydroxyethyl)piperazine-1-ethanesulfonic acid; MR, mandelate racemase; VDW, van der Waals.

Scheme 1 ^a

^a B₁ and B₂ represent the active site bases His 297 and Lys 166, respectively.

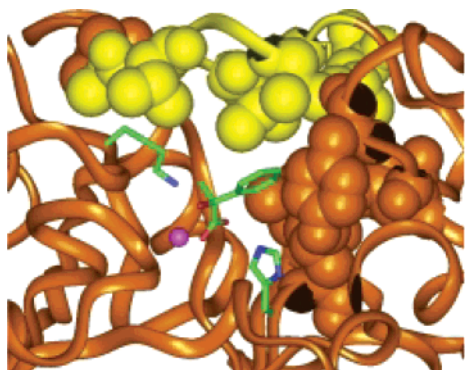


FIGURE 1: X-ray crystal structure of the active site hydrophobic cavity of wild-type MR with bound (*S*)-atrolactate [PDB code 1MDR (6)]. The general acid/base catalysts (His 297 and Lys 166) are shown along with the essential Mg^{2+} ion. Space-filling representations of residues making up the hydrophobic pocket (Phe 52, Tyr 54, Leu 142, Leu 298, Leu 319, and Leu 321) within the α/β -barrel are displayed in gold and are drawn at the VDW radii. Hydrophobic residues contributed by the flexible hinged loop are shaded yellow (Leu 18, Val 22, Ala 25, Val 26, and Val 29).

or transition state by delocalization of negative charge into a β,γ -unsaturated system contributes significantly to catalysis (18, 19, 23). While the structure of the hydrophobic cavity within the active site of MR has been well characterized and the requirement for β,γ -unsaturation in catalysis is clear, the contribution to catalysis from enzyme–ligand interactions within the hydrophobic cavity has not been clearly established.

MR is extremely proficient at discriminating between the substrate in the ground state and the altered substrate in the transition state, binding the latter with an apparent association constant equal to approximately $5 \times 10^{18} \text{ M}^{-1}$ thereby stabilizing the transition state by 26 kcal/mol (24). Highly proficient enzymes are often strongly inhibited by analogues of either the altered substrate in the transition state or unstable intermediates that resemble the transition state (25–27). Indeed, we have shown that benzohydroxamate is a potent intermediate analogue inhibitor of MR, binding with an affinity that is 2 orders of magnitude greater than that observed for the substrate (8). Using N197A MR, we demonstrated that the binding of benzohydroxamate is more sensitive to changes in transition state binding free energy than to changes in substrate binding free energy, and hence benzohydroxamate may be regarded as a transition state analogue (8).

The high proficiency of MR is achieved principally by enthalpy reduction, with enthalpy providing nearly 23 kcal/mol to the apparent binding free energy of the altered substrate in the transition state (20). This substantial release of energy is compatible with the development of enhanced

hydrogen bonding, electrostatic interactions, and nonpolar interactions in the enzyme–transition state complex (28). While it is clear that numerous electrostatic interactions between the ligand and polar residues within the active site contribute to transition state stabilization (5–8, 24, 29, 30), it is also possible that nonpolar interactions originating in the hydrophobic cavity may contribute to stabilization of the altered substrate in the transition state.

In the present work, we examine binding interactions between the hydrophobic cavity and a series of ground state (glycolates) and intermediate (hydroxamates) analogues. We demonstrate that the free energy changes accompanying binding of MR with both substrate and intermediate analogues bearing alkyl groups in place of the phenyl group (π) and the VDW surface areas of the ligands. Interestingly, the intermediate analogue benzohydroxamate is bound 2 orders of magnitude more tightly than would be predicted on the basis of these correlations, suggesting that specific enzyme–ligand interactions stabilize the enolic intermediate of mandelate relative to the ground state. We also use the alternative substrate 2-naphthylglycolate and the corresponding intermediate analogue, 2-naphthohydroxamate, to show that steric constraints within the hydrophobic cavity of the MR–intermediate complex are more stringent than those in the MR–substrate complex.

MATERIALS AND METHODS

Racemic (*R*)- and (*S*)-mandelic acid, (*R*)- and (*S*)-hexahydromandelic acid, (*R*)- and (*S*)-lactic acid, (*S*)-(-)-2-hydroxy-3,3-dimethylbutyric acid, glycolic acid, acetohydroxamic acid, benzohydroxamic acid, and (*R*)- and (*S*)- α -methylbenzylamine were purchased from Sigma-Aldrich Canada Ltd. (Oakville, Ontario, Canada). All other reagents were purchased from Sigma-Aldrich Canada Ltd. Recombinant MR from *Ps. putida* was overexpressed in and purified from *Escherichia coli* strain BL21(DE3) cells transformed with a pET15b plasmid (Novagen, Madison, WI) containing the MR gene (8). This construct encodes the MR gene product with an N-terminal polyhistidine tag [MGSS(H)₆SSGLV-PRGSHM₁...MR]. The enzyme was purified by metal ion affinity chromatography as described previously (8). The presence or absence of the hexahistidine tag does not influence the kinetic parameters for the recombinant enzyme (31). Melting points (uncorrected) were determined on a Gallenkamp melting point apparatus, and optical rotations at 589 nm were measured using a Rudolph Instruments Digipol 781 automatic polarimeter. NMR spectra were obtained using a Bruker AC 250F spectrometer. Chemical shifts are reported relative the deuterium lock signal calibrated for the indicated deuterated solvent. Circular dichroism

assays were conducted using a JASCO J-810 spectropolarimeter. Elemental analyses were conducted by Canadian Microanalytical Service Ltd. (Delta, British Columbia, Canada).

(*R,S*)-1-Naphthylglycolic Acid. The preparation of (*R,S*)-1-naphthylglycolic acid was based on the synthesis of mandelic acid from benzaldehyde described by Maggio et al. (32). 1-Naphthaldehyde (15.62 g, 0.1 mol) was added to a solution of sodium bisulfite (11 g, 0.1 mol) in water (30 mL), and the mixture was swirled vigorously for 20 min. Potassium cyanide (14 g, 0.2 mol) dissolved in water (30 mL) was then added, and the mixture was swirled vigorously for an additional 20 min. A yellow-orange oil separated, and the resulting solution was extracted with ether. The ether extract was washed with water and twice with a saturated sodium chloride solution. After the ether extract was dried over magnesium sulfate, the ether was removed by rotary evaporation, leaving an orange oil. The oil (4 g) was added dropwise to hot hydrochloric acid (5.3 M). After being refluxed for 3 h, the solution was cooled to room temperature, and any unreacted brown oil was removed using a disposable pipet. The solution was then extracted twice with ether, and the combined ether extracts were dried over magnesium sulfate. Removal of the ether by rotary evaporation gave a crude product that was recrystallized from benzene to yield silver-brown crystals of racemic 1-naphthylglycolic acid (1.12 g, 25% yield): mp 89–92 °C [lit. 87–88 °C (33)]; ^1H NMR δ (250.13 MHz; CDCl_3 , ppm) 5.81 (1 H, s), 7.28–8.31 (7 H, m). Anal. Calcd for $\text{C}_{12}\text{H}_{10}\text{O}_3$: C, 71.28; H, 4.98. Found: C, 71.16; H, 5.02.

(*R,S*)-2-Naphthylglycolic Acid. Racemic 2-naphthylglycolic acid was prepared according to the procedure described by Compere (33). 1,4-Dioxane (100 mL), 2-naphthaldehyde (15.6 g, 0.1 mol), and bromoform (25.24 g, 0.1 mol) were added to a slurry of lithium chloride (8.48 g, 0.2 mol), potassium hydroxide (23.6 g, 0.4 mol), and ice (100 g). After being stirred for 24 h at 4 °C, the pH was adjusted to 12 by addition of potassium hydroxide (6 M, 8 mL), and the solution was stirred for an additional 24 h at 37 °C. The solution was then diluted with water (100 mL), acidified with concentrated HCl (20 mL), and extracted twice with ether (50 mL). The combined ether extracts were washed with a saturated sodium chloride solution and dried over magnesium sulfate. An orange solid remained after the ether was removed using rotary evaporation. Recrystallization from chloroform–hexanes–ethanol (8:2:1) afforded white needles of racemic 2-naphthylglycolic acid (9.6 g, 48% yield): mp 148–150 °C [lit. 155–156 °C (33), 163.5–167 °C (34)]; ^1H NMR δ (250.13 MHz; CD_3OD , ppm) 5.31 (1 H, s), 7.45–7.86 (7 H, m). Anal. Calcd for $\text{C}_{12}\text{H}_{10}\text{O}_3$: C, 71.28; H, 4.98. Found: C, 70.54; H, 4.94.

Resolution of (*R*)- and (*S*)-2-Naphthylglycolic Acid. Both (*R*)- and (*S*)-2-naphthylglycolic acid were resolved using the procedure of Kinbara et al. (34). (*R*)-(+)- α -Methylbenzylamine (3.44 mL, 26.8 mmol) was added to a solution of (*R,S*)-2-naphthylglycolic acid (5.4 g, 26.8 mmol) in ethanol (150 mL). The solution was refluxed for 30 min and then slowly cooled to room temperature. Crystals (5.90 g) that appeared after 2 days were subsequently recrystallized twice from aqueous ethanol (90%). The resulting salt was dissolved in water (100 mL). Upon acidification of this solution with aqueous HCl (3 M, 50 mL), a white precipitate formed. The

solid and aqueous phase were extracted four times with ether (100 mL), and the combined ether extracts were dried over magnesium sulfate. Removal of the ether by rotary evaporation gave a white powder. Recrystallization of this crude product from chloroform–ethanol (10:1) afforded pure (*R*)-2-naphthylglycolic acid (0.32 g, 6% yield): $[\alpha]^{20}_{\text{D}} = -144.9$ ($c = 1.7$, EtOH) [lit. $[\alpha]^{20}_{\text{D}} = -145.6$ ($c = 0.98$, EtOH) (34), $[\alpha]^{21}_{\text{D}} = -142.2$ ($c = 0.98$, EtOH) (35)].

(*S*)-2-Naphthylglycolic acid was resolved by addition of (*S*)-(-)- α -methylbenzylamine (3.70 mL, 28.8 mmol) to a solution of (*R,S*)-2-naphthylglycolic acid (5.8 g, 28.8 mmol) in ethanol (100 mL). The solution was refluxed for 30 min and then slowly cooled to room temperature. Crystals (4.37 g) that appeared after 24 h were subsequently recrystallized twice from aqueous ethanol (90%). Crude (*S*)-2-naphthylglycolic acid was liberated from the salt as described for (*R*)-2-naphthylglycolic acid and recrystallized from chloroform–ethanol (15:1) to afford pure (*S*)-2-naphthylglycolic acid (94.1 mg, 2% yield): $[\alpha]^{20}_{\text{D}} = +146.8$ ($c = 0.8$, EtOH) [lit. $[\alpha]^{20}_{\text{D}} = +144.7$ ($c = 0.98$, EtOH) (34), $[\alpha]^{21}_{\text{D}} = +142.5$ ($c = 0.98$, EtOH) (35)].

2-Naphthohydroxamic Acid. 2-Naphthohydroxamic acid was prepared according to the procedure described by Summers et al. (36). 2-Naphthoic acid (2.5 g, 14.5 mmol) was dissolved in dichloromethane (100 mL) containing DMF (1.06 g, 14.5 mmol). The solution was cooled to 0 °C, and oxalyl chloride (4.4 g, 32.6 mmol) was added dropwise. After being stirred for 45 min, this solution was added to a solution of hydroxylamine hydrochloride (3.75 g, 58 mmol) and triethylamine (8.8 g, 87 mmol) in THF–water (5:1, 60 mL) while the temperature was maintained at 0 °C. The solution was stirred for an additional 30 min at 25 °C and poured into aqueous HCl (2 M, 100 mL), and the resulting acidic solution was then extracted with dichloromethane (200 mL). A precipitate formed rapidly in dichloromethane and was collected by suction filtration and recrystallized from ethanol (100%) to afford colorless needles of 2-naphthohydroxamic acid (400 mg, 15% yield): mp 162–164 °C [lit. 169–170 °C (36)]; ^1H NMR δ (250.13 MHz; CD_3OD , ppm) 7.5–8.25 (m). Anal. Calcd for $\text{C}_{11}\text{H}_9\text{NO}_2$: C, 70.58; H, 4.85; N, 7.48. Found: C, 70.51; H, 5.11; N, 7.49.

Cyclohexanecarbohydroxamic Acid. Methyl cyclohexanecarboxylate was reacted with (*O*-benzylhydroxylamino)-methylaluminum chloride on a 10 mmol scale to generate the *O*-(benzylcyclohexyl)hydroxamate according to the general procedure described by Pirrung and Chau (37). The crude *O*-(benzylcyclohexyl)hydroxamate was a yellow oil. Silica chromatography using hexanes–ethyl acetate (3:1) as the mobile phase afforded a white crystalline product. The *O*-benzylhydroxamate (117 mg, 0.5 mmol) was subsequently dissolved in methanol (20 mL) and hydrogenated over palladium for 14 h according to the procedure described by Pirrung and Chau (37). The resulting white powder was recrystallized from hexanes–ethyl acetate (3:1) to give cyclohexanecarbohydroxamic acid as white needles (40.7 mg, 3% yield): mp 119–120 °C [lit. 125–129 °C (37), 137–139 °C (38)]; ^1H NMR δ (250.13 MHz; D_2O , ppm) 1.14–2.19 (m). Anal. Calcd for $\text{C}_7\text{H}_{13}\text{NO}_2$: C, 58.71; H, 9.15; N, 9.78. Found: C, 59.51; H, 9.24; N, 9.91.

Trimethylacetohydroxamic Acid. Trimethylacetohydroxamic acid was synthesized according to the general method described by Larsen et al. (39). Sodium hydroxide (4.3 g,

0.11 mol) and methyl trimethylacetate (13.3 mL, 0.10 mol) were added to a solution of hydroxylamine hydrochloride (6.95 g, 0.10 mol) in methanol (100 mL). The mixture was stirred at room temperature for 3 days, and formation of the hydroxamate was verified by the development of a characteristic purple spot on a silica plate after treatment with aqueous ferrous chloride. The solution was adjusted to pH 7 by addition of methanolic HCl, filtered, and evaporated to dryness. The crude mixture was extracted three times with ethyl acetate (25 mL), and the combined extracts were evaporated to dryness. Recrystallization from toluene–petroleum ether (1:1, 100 mL, with a few drops of ethanol) afforded pure trimethylacetohydroxamic acid as colorless needles (0.90 g, 9% yield): mp 153–155 °C [lit. 154–159 °C (40), 160–161 °C (41)]; ^1H NMR δ (250 MHz; D_2O , ppm) 1.18 (s). Anal. Calcd for $\text{C}_5\text{H}_{11}\text{NO}_2$: C, 51.26; H, 9.46; N, 11.96. Found: C, 50.90; H, 9.35; N, 11.87.

Propionohydroxamic Acid. Propionohydroxamic acid was synthesized according to the general methods described by Larsen et al. (39) and Fishbein et al. (42). Sodium hydroxide (4.3 g, 0.11 mol) and ethyl propionate (10.21 g, 0.10 mol) were added to a solution of hydroxylamine hydrochloride (6.95 g, 0.10 mol) in methanol (100 mL). The mixture was stirred at room temperature for 36 h, and formation of the hydroxamic acid was verified as described above. The solution was adjusted to pH 6 by addition of methanolic HCl, filtered, and evaporated to yield a yellow oil. Methanol (100 mL) was added, and again, the solution was evaporated to yield a yellow oil and some crystals. This crude mixture was extracted with boiling ethyl acetate (100 mL) and hot filtered. The volume of the filtrate was reduced by boiling to ~10 mL, and acetone (2 mL) was added. Crystallization overnight at room temperature afforded pure propionohydroxamic acid as colorless needles (1.54 g, 17% yield): mp 90–95 °C [lit. 92–96 °C (42), 91–92 °C (43)]; ^1H NMR δ (250.13 MHz; D_2O , ppm) 1.06–1.12 (t, 3H, $J = 7.5$ Hz), 2.11–2.54 (q, 2H, $J = 7.5$ Hz). Anal. Calcd for $\text{C}_3\text{H}_7\text{NO}_2$: C, 40.44; H, 7.92; N, 15.72. Found: C, 40.62; H, 7.57; N, 15.58.

Enzyme Assay. MR activity was assayed using the circular dichroism (CD) assay described by Sharp et al. (44). All inhibition assays were conducted at 25 °C in Na^+ -HEPES buffer (0.1 M, pH 7.5) containing MgCl_2 (3.3 mM) and bovine serum albumin (BSA, 0.1%). For all inhibition assays, the conversion of (*R*)-mandelate to (*S*)-mandelate was followed, and the concentrations of (*R*)-mandelate ranged from 0.24 to 9.50 mM. Reactions were initiated by addition of MR to give a final enzyme concentration between 150 and 250 ng/mL. Except where mentioned otherwise, initial velocities were determined by following the change in ellipticity at 262 nm in a quartz cuvette with a 1 cm light path. Inhibition assays with 1-naphthylglycolic acid and 2-naphthylglycolic acid were conducted at 262 nm using a quartz cuvette with a 0.5 cm light path. The commercial preparation of (*S*)-(–)-2-hydroxy-3,3-dimethylbutyric acid was very hygroscopic, and hence to accurately determine its concentration in inhibition assays, NMR was used to quantify the α -hydrogen peak of (*S*)-(–)-2-hydroxy-3,3-dimethylbutyric acid relative to a benzoic acid standard. For inhibition assays with 2-naphthohydroxamate, 20% DMSO was added to the 0.1 M Na^+ -HEPES buffer to increase the solubility of the inhibitor. The addition of 20% DMSO to the assay buffer altered the molar ellipticity of (*R*)-mandelate

at 262 nm ($[\theta]_{262}^R = +2908 \text{ deg mol}^{-1} \text{ cm}^2$) but had no effect on the K_m for (*R*)-mandelate [0.8 ± 0.1 mM in 0% DMSO (8); 1.0 ± 0.3 mM in 20% DMSO] or on the K_i for benzohydroxamate [$11.7 \mu\text{M}$ in 0% DMSO (8); $11.8 \mu\text{M}$ in 20% DMSO].

For assays with the substrates (*R*)- and (*S*)-2-naphthylglycolic acid, the reactions were followed at 266 nm ($[\theta]_{266}^R = -35000 \text{ deg mol}^{-1} \text{ cm}^2$) in a quartz cuvette with a 0.1 cm light path. Reactions were initiated by addition of MR to give a final enzyme concentration between 0.5 and 2.0 $\mu\text{g/mL}$.

Data Analysis. The values of V_{\max} and K_m were determined from plots of the initial velocity (v_i) versus substrate concentration ($[\text{S}]$) by fitting the data to eq 1 using nonlinear regression analysis and the program EnzymeKinetics v1.5b5 (Trinity Software, Plymouth, NH). Competitive inhibition constants (K_i) were determined from linear replots of the observed values of K_m/V_{\max} versus inhibitor concentration ($[\text{I}]$) according to eq 2. All kinetic parameters were determined in triplicate, and average values are reported. The reported errors are standard deviations. Protein concentrations were determined using the Bio-Rad protein assay (Bio-Rad Laboratories, Mississauga, Ontario, Canada) with BSA standards, and k_{cat} values were obtained by dividing V_{\max} values by the total enzyme concentration ($[\text{E}]_t$) using M_r 40728.

$$v_i = \frac{V_{\max}[\text{S}]}{K_m + [\text{S}]} \quad (1)$$

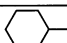
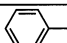


$$v_i = \frac{V_{\max}[\text{S}]}{K_m(1 + [\text{I}]/K_i) + [\text{S}]} \quad (2)$$

Computer Modeling. Geometry optimizations and van der Waals (VDW) surface areas were calculated for glycolate, (*S*)-lactate, (*S*)- α -hydroxybutyrate, (*S*)-2-hydroxy-3,3-dimethylbutyrate, (*S*)-mandelate, (*S*)-hexahydromandelate, and the *trans*-conjugate bases of benzohydroxamic acid, aceto-hydroxamic acid, trimethylacetohydroxamic acid, propionohydroxamic acid, naphthohydroxamic acid, and cyclohexanecarboxhydroxamic acid by conducting self-consistent field calculations at the 6-31G* level using MacSpartan Plus software (Wavefunction, Inc., Irvine, CA). VDW surface areas are based on an electron density isosurface with a density of 0.002 e/b³, which encompasses approximately 95% of the VDW radii (45).

RESULTS AND DISCUSSION

Enzymes utilize many interactive forces, including hydrogen bonding, electrostatic interactions, VDW forces, and entropically driven hydrophobic interactions to bind substrates and stabilize transition states and intermediates during catalysis (46). For MR, such interactions include hydrogen bonding with Glu 317 (6, 7) and Asn 197 (8) and electrostatic interactions with Lys 164 (16) and Mg^{2+} (6, 30, 47). The importance of these polar interactions is underscored by the major enthalpic contribution that they make to transition state stabilization (20). However, the contribution of hydrophobic interactions to catalysis is less well understood probably because no distinct point of interaction can be readily identified. The hydrophobic cavity of MR, for example, is

Table 1: Competitive Inhibition Constants for Mandelate Racemase with Substrate and Intermediate Analogues and Their Pieces

R	$\begin{array}{c} \text{O}=\text{C}-\text{O}^- \\ \\ \text{H}-\text{C}-\text{OH} \\ \\ \text{R} \\ \text{glycolate} \end{array}$	$\begin{array}{c} \text{N}=\text{OH} \\ \\ \text{C}-\text{OH} \\ \\ \text{R} \\ \text{hydroxamic acid}^a \end{array}$
H-	$K_i = 30.2 \pm 5.7 \text{ mM}$	
	$\begin{array}{c} (R) \\ K_i, \text{mM} \\ (\Delta\Delta G, \text{kcal/mol}) \end{array}$	$\begin{array}{c} (S) \\ K_i, \text{mM} \\ (\Delta\Delta G, \text{kcal/mol}) \end{array}$
CH ₃ -	32.0 ± 1.4 (0.03 ± 0.01) ^b	26.1 ± 3.1 (-0.09 ± 0.02) ^b
CH ₃ CH ₂ -	3.6 ± 0.4 (for (R,S) ^c) (-1.3 ± 0.3) ^b	
(CH ₃) ₃ C-	—	1.39 ± 0.27 (-1.8 ± 0.5) ^b
	0.70 ± 0.24 (-2.2 ± 0.9) ^b	0.071 ± 0.029 (-3.6 ± 1.6) ^b
	0.84 ± 0.04 (-2.1 ± 0.4) ^b	0.73 ± 0.05 (-2.2 ± 0.4) ^b
Substrate Analogue Pieces Lacking the Carboxyl Function		
	$K_i = 15.4 \pm 1.9 \text{ mM}$	
		$K_i \geq 230 \text{ mM}^e$ $K_i \geq 950 \text{ mM}^f$

^a The hydroxamate is drawn as the enol because it resembles the putative enolic intermediate and an OH function is required at the α -position for potent inhibition (8). (The cis arrangement shown is an arbitrary choice.) ^b Binding free energy due to the glycolate R group; i.e., $\Delta\Delta G = -RT \ln(K_i^H/K_i^R)$. ^c Value from ref 23. ^d Binding free energy due to the hydroxamate R group; i.e., $\Delta\Delta G = -RT \ln(K_i^{\text{CH}_3}/K_i^R)$. ^e K_i value estimated assuming competitive inhibition and a limit of $\geq 5\%$ detectable loss of activity in the presence of the inhibitor. ^f K_i value estimated assuming noncompetitive inhibition and a limit of $\geq 5\%$ detectable loss of activity in the presence of the inhibitor.

likely to contribute a set of diffuse VDW forces that serve to bind the phenyl group of the substrate. But how significant are hydrophobic interactions in substrate binding and transition state stabilization? To address this question, we have determined the competitive inhibition constants for a series of glycolates (substrate analogues) and hydroxamates (intermediate analogues) and constructed linear free energy relationships describing the dependence of the binding affinity on hydrophobicity and VDW surface areas.

Substrate Analogue Binding. Comparison of the binding constants of (*R*)- and (*S*)-mandelate with that of either glycolate, (*R*)-lactate, or (*S*)-lactate reveals that interactions between the hydrophobic pocket and the phenyl group contribute ~ 2 kcal/mol of free energy to ground state binding (Table 1). Comparison of the binding constants for mandelate with those for glycolate and benzyl alcohol reveals that the phenyl group and the carboxylate group make approximately equal contributions to the binding affinity in the ground state (2.1 kcal/mol vs 1.8 kcal/mol, respectively; cf. ref 23).

Contributions to the free energy for binding of the substrate in the hydrophobic cavity could originate from several sources, including entropically driven hydrophobic interactions, specific electrostatic interactions, and VDW forces. It is unlikely, however, that specific electrostatic interactions such as π - π interactions (48) or cation- π interactions (49) contribute significantly to ground state binding since substrate analogues with bulky alkyl groups in place of the phenyl ring (e.g., hexahydromandelate and *tert*-butylglycolate) exhibit binding affinities similar to that of mandelate. If the active site of MR "solvates" the substrate similar to a nonpolar solvent, then the free energy changes associated with the binding of substrate and substrate analogues should

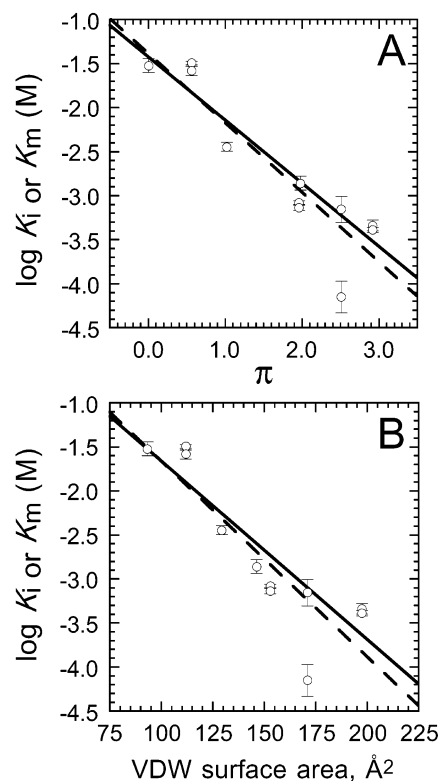


FIGURE 2: Correlation between $\log K_i$ values for the modified glycolate inhibitors and the hydrophobicity substituent constant π (A) and VDW surface areas (B). (A) Values of π are for substituents on the β -carbon atom of the substrates/inhibitors and are from ref 56 except for the value corresponding to the naphthyl group, which was calculated from $\log P_{\text{C}_{10}\text{H}_8} - \log P_{\text{H}_2}$ (75, 76). The dotted linear regression line includes all values (slope = -0.79 ± 0.11 , $r^2 = 0.844$) while the point corresponding to (*S*)-hexahydromandelate is omitted in the solid linear regression line (slope = -0.72 ± 0.08 , $r^2 = 0.915$). (B) The VDW surface areas were calculated as described in Materials and Methods. The dotted linear regression line includes all values (slope = $-0.022 \pm 0.004 \text{ \AA}^{-2}$, $r^2 = 0.769$) while the point corresponding to (*S*)-hexahydromandelate is omitted in the solid linear regression line (slope = $-0.020 \pm 0.003 \text{ \AA}^{-2}$, $r^2 = 0.853$).

be proportional to their corresponding free energy changes for partitioning between nonpolar solvents and water (50–55). Indeed, a plot of the log of the binding constants (K_s for mandelate and 2-naphthylglycolate and the K_i values for substrate analogues) against π , the hydrophobicity substituent constant based on partitioning coefficients between octanol and water (56), is linear [slope = -0.72 ± 0.08 (Figure 2)]. This suggests that the hydrophobic cavity of MR effectively solvates the phenyl group of the substrate in an environment that is slightly less hydrophobic than octanol. Interestingly, the free energy change accompanying (*S*)-hexahydromandelate binding is about 10-fold greater than that of the *R* enantiomer or what would be predicted using the regression line. This “anomaly” may arise from fortuitous interactions within the hydrophobic cavity. Such enantioselectivity has been reported previously for the enantiomers of α -hydroxybenzylphosphonate (8), α -fluorobenzylphosphonates (57), atrolactate, and the irreversible inactivator α -phenylglycidate (6).

Hydrophobic effects arise primarily from favorable changes in free energy that accompany the release of ordered water molecules surrounding a hydrophobic surface to bulk solvent. Consequently, the hydrophobic effect correlates with the area

of the hydrophobic surface that is desolvated (25). Hence, the free energy changes associated with ligand binding to MR should correlate with the VDW surface area of the ligands (25, 58–60). Figure 2B shows a plot of $\log K_i$ values for the series of glycolates against their corresponding VDW surface areas. The slope of the solid line in Figure 2B ($-0.022 \pm 0.004 \text{ \AA}^{-2}$) can be converted to a free energy dependence [i.e., $\Delta G/\text{surface area} = 2.303RT(\text{slope})$] equal to $-30 \pm 5 \text{ cal mol}^{-1} \text{ \AA}^{-2}$ at 25 °C. This value is in the range generally accepted for desolvated hydrophobic surfaces [$25\text{--}30 \text{ cal mol}^{-1} \text{ \AA}^{-2}$ (25, 58–61)].

Intermediate Analogue Binding. The phenyl group of mandelate contributes to catalysis by acting as an electron sink to stabilize the enolic intermediate. Our observation that (*S*)-hexahydromandelate (20 mM) shows no detectable change in CD signal after a 48 h incubation with MR (20 $\mu\text{g/mL}$) and the observation by Li et al. (23) that vinylglycolate is a substrate for MR, while ethylglycolate is not, support the notion that β,γ -unsaturation is required for catalysis. Is this the only contribution that the phenyl group makes to catalysis or do other interactions within the hydrophobic cavity also contribute to catalysis through stabilization of the intermediate and transition states?

In previous work, we reported that the intermediate analogue benzohydroxamate is a potent competitive inhibitor of MR, binding with an affinity approximately 100-fold greater than that observed for the substrate (8). Benzohydroxamate shares geometric and electronic features with the putative *aci*-carboxylate intermediate formed during MR catalysis (Scheme 1), including an sp^2 -hybridized α -carbon. Examination of the linear free energy relationship between the apparent binding affinity of intermediate analogues (Table 1) and their hydrophobicity (π values) and VDW surface areas reveals good correlation for hydroxamate derivatives of alkanolic acids and 2-naphthoic acid (Figure 3). The slope of the line in Figure 3A is -1.13 ± 0.05 , indicating that the hydrophobic cavity of MR solvates the phenyl group of the intermediate in an environment that is slightly more hydrophobic than octanol. The slope of the line in Figure 3B ($-0.030 \pm 0.002 \text{ \AA}^{-2}$) gives a free energy dependence equal to $-41 \pm 3 \text{ cal mol}^{-1} \text{ \AA}^{-2}$ at 25 °C. This free energy dependence is about $10 \text{ cal mol}^{-1} \text{ \AA}^{-2}$ greater than that observed for ground state binding, indicating that MR exhibits a marginally enhanced hydrophobic interaction with the intermediate relative to the substrate during catalysis. It is interesting to note that the free energy change associated with the binding of benzohydroxamate exceeds that which would be predicted solely on the basis of the correlation of $\log K_i$ values with either π values or VDW surface areas by approximately 2 orders of magnitude (i.e., $\sim 2.5 \text{ kcal/mol}$). Comparison of the inhibition constant for benzohydroxamate with that of acetohydroxamate reveals a contribution from the phenyl substituent of 4.6 kcal/mol to the overall binding free energy of the intermediate analogue. This is more than twice the energy contributed by the phenyl substituent to *substrate* binding (vide supra). Neither the *tert*-butyl- nor the cyclohexyl-substituted hydroxamates capture greater than 3 kcal/mol in binding free energy relative to acetohydroxamate, emphasizing that there exists a marked preference for binding of the phenyl substituent of the intermediate analogue over that predicted from solely hydrophobic interactions. These observations suggest that, in addition to

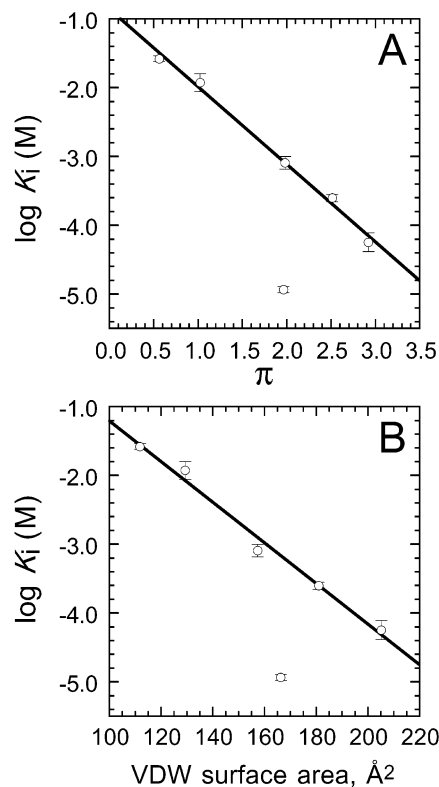
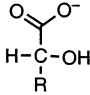
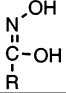


FIGURE 3: Correlation between $\log K_i$ values for the hydroxamate inhibitors and the hydrophobicity substituent constant π (A) and VDW surface areas (B). (A) Values of π were obtained as described in Figure 2 and are for substituents on the carbon atom of the hydroxamate function. The linear regression line shown uses all data points except for that corresponding to benzohydroxamate (slope = -1.13 ± 0.05 , $r^2 = 0.994$). (B) The VDW surface areas were calculated as described in Materials and Methods. The linear regression line shown uses all data points except for that corresponding to benzohydroxamate (slope = $-0.030 \pm 0.002 \text{ \AA}^{-2}$, $r^2 = 0.987$).

slightly enhanced hydrophobic interactions that accompany intermediate analogue binding relative to substrate binding, other specific interactions are involved in binding the phenyl group of the intermediate. In addition, this specific interaction requires that the polar end of either the substrate or the intermediate must be present since benzene did not inhibit MR and benzyl alcohol was only a weak competitive inhibitor (Table 1).

Why is binding of the phenyl group favored in the planar intermediate and not in the ground state? The stability constants for the complexes of the divalent metal ions Cu^{2+} , Ni^{2+} , Zn^{2+} , Ca^{2+} , and Mg^{2+} with acetohydroxamate, cyclohexanohydroxamate, and benzohydroxamate are very similar (62) and cannot account for the difference of 3 orders of magnitude observed between the binding affinities of acetohydroxamate and benzohydroxamate. The pK_a values for the conjugate acids of acetohydroxamate, cyclohexanohydroxamate, and benzohydroxamate are also very similar (62), precluding any effects on the inhibition constants due to differences in ionization states. Our observations suggest that some ($\sim 1 \text{ kcal/mol}$) of the increased binding energy for the phenyl group in the enzyme–intermediate complex arises from the slightly enhanced hydrophobic interactions within the active site. Such an effect could arise from enhanced complementarity between the hydrophobic residues of the flexible hinged loop over the active site (17) and the phenyl

Table 2: Kinetic Constants for MR-Catalyzed Racemization of Mandelate and 2-Naphthylglycolate and Inhibition by Naphthylglycolates and 2-Naphthohydroxamate

Substrate Kinetic Parameters		
		
	R = phenyl	R = 2-naphthyl
$K_m^{(R)}$ (mM)	0.81 ± 0.12	0.46 ± 0.06
$K_m^{(S)}$ (mM)	0.62 ± 0.04	0.41 ± 0.03
$k_{cat}^{(R) \rightarrow (S)}$ (s^{-1})	514 ± 48	33 ± 1
$k_{cat}^{(S) \rightarrow (R)}$ (s^{-1})	447 ± 12	25 ± 1
Inhibition Constants		
(R,S)-1-naphthylglycolate, K_i (mM)		1.9 ± 0.1
(R,S)-2-naphthylglycolate, K_i (mM)		0.52 ± 0.03
		
	R = phenyl	R = 2-naphthyl
K_i (μ M)	12 ± 1	57 ± 18

group of the intermediate (i.e., increased VDW forces) and possibly additional weak polar interactions (48). For example, the hydrophobic pocket of neurophysin exhibits an unusually large (5.1 kcal/mol) difference in binding energies between Phe and Leu at position 2 of peptide ligands. Modeling studies using crystallographic data indicate that this difference in binding energies arises from a 3.4 kcal/mol difference in packing energies. The bound Leu side chain is only able to establish one-third of the VDW contacts available to the Phe side chain, despite only a $\sim 17\%$ difference in accessible surface areas between the two side chains (60, 63). In addition, weak polar interactions with backbone nitrogens and side chain sulfurs may contribute an additional 4 kcal/mol of binding energy (64). Interestingly, the binding of cyclohexane within the same hydrophobic pocket of neurophysin is disfavored as a result of steric hindrance (64). In order for similar advantageous and specific interactions to occur between the phenyl group of the planar intermediate and the active site of MR, there must be a relatively high degree of complementarity between the active site and the aromatic ring. Similar studies on a hydrophobic cavity in γ -glutamylcysteine synthetase (65) revealed that a nonpolar substrate Cys residue and a substrate carboxylate group made equal contributions to transition state stabilization, demonstrating that nonpolar interactions can play a significant role in enzyme-transition state stabilization.

It is clear from our analysis that hydrophobic effects alone cannot account for the preferred binding of the phenyl group relative to alkyl groups in the intermediate analogues. X-ray crystal structures of wild-type and mutant forms of MR with bound substrate or substrate analogues (5–7, 16, 17) do not suggest any obvious side chains of amino acid residues that could interact with the phenyl group of the intermediate through aromatic stacking interactions. It is possible that the two general acid/base catalysts in the active site may serve

as potential partners in either cation- π interactions (66) or hydrogen bonding-type interactions (67) with the phenyl group of the intermediate.² Abstraction of the α -proton from either (R)- or (S)-mandelate to generate the enolic intermediate will leave MR with both His 297 and Lys 166 existing as their conjugate acids. If the crystal structure of the unliganded enzyme (17) or the enzyme-substrate/analogue complexes (5–7, 16) approximates that of the enzyme-intermediate complex, then the distance between the protonated forms of His 297 and Lys 166 should be ~ 6.7 – 8.5 Å. Positioning the phenyl group between these positive charges would yield a distance of ~ 3.8 Å between the phenyl group and the positive charges on either side. This distance is similar to that observed for most cation- π interactions in proteins [i.e., ≤ 4.0 Å (66)], and such an interaction (e.g., His 297⁺/aromatic) might contribute 0.3–0.5 kcal/mol or greater to the free energy of binding (68–70). We are currently pursuing crystallographic studies of MR complexed with benzohydroxamate to explore these possibilities.

Finally, we note the possibility that dehydration of the hydrophobic pocket could also play a role in the free energy changes accompanying ligand binding. However, the VDW volumes of the phenyl and *tert*-butyl groups are similar (71), and hence each group should displace water molecules to a similar extent.

Racemization of 2-Naphthylglycolate. As part of our survey of the interaction of substrate and intermediate analogues with MR, we found that (R,S)-1-naphthylglycolate and (R,S)-2-naphthylglycolate were competitive inhibitors of MR with respect to (R)-mandelate, binding to the enzyme with approximately the same affinity as (R)- or (S)-mandelate (Table 2). Despite the fact that MR exhibited an apparent affinity for (R,S)-1-naphthylglycolate that was 4-fold less than that exhibited for (R,S)-2-naphthylglycolate (probably due to unfavorable steric interactions between the C5–C10 portion of the naphthyl ring and the protein), replacement of the phenyl group of mandelate with a naphthyl group seemed to be well tolerated by the hydrophobic pocket.

Because there appear to be slightly enhanced VDW forces between MR and the phenyl group of mandelate in the enzyme-intermediate complex, we reasoned that racemization of 2-naphthylglycolate might exhibit a sensitivity to steric interactions. As shown in Table 2, the K_m values for both (R)- and (S)-2-naphthylglycolate are slightly less than those for (R)- and (S)-mandelate while the k_{cat} values are approximately 6% of the k_{cat} values observed for (R)- and (S)-mandelate. Because $K_m \approx K_S$ for MR (20), it is clear that the enzyme binds 2-naphthylglycolate and mandelate with equal affinity and, in contrast to the suggestion by Felfer et al. (18), no steric restrictions are imposed on the binding of the bulkier substrate in the ground state. The observed 10-fold decrease in k_{cat}/K_m for 2-naphthylglycolate relative to mandelate is caused by an increase in the free energy barrier for the chemical steps as shown in Figure 4. The extended π system of 2-naphthylglycolate should stabilize a negative charge on the α -carbon through resonance slightly better than the phenyl group [e.g., the value of σ_{para}

² We thank Professor John Gerlt for suggesting the possible role of the conjugate acids of the two active site general acid/base catalysts in stabilizing the intermediate.

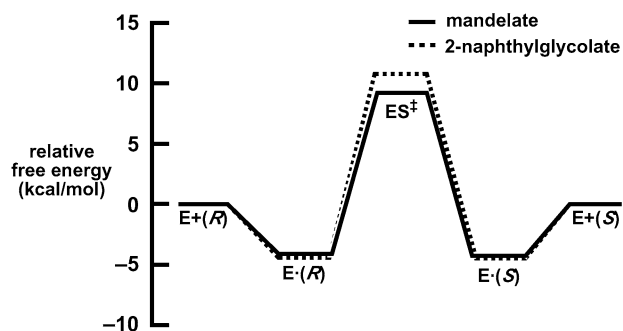


FIGURE 4: Free energy profiles (25 °C, pH 7.5) for the racemization of (*R*)- and (*S*)-mandelate (solid line) and (*R*)- and (*S*)-2-naphthylglycolate (dashed line) catalyzed by MR. The *R* and *S* substrate enantiomers are denoted as (*R*) and (*S*), respectively. The profiles were derived from the kinetic parameters given in Table 2 and assuming a standard state of 1 M. ES⁺ represents the enzyme–substrate complex in the transition state.

is 0.042 (72) and σ_{para}^+ ranges between -0.14 and -0.28 (73) for the 2-naphthyl substituent, while the value of σ_{para} is -0.01 and σ_{para}^+ is -0.179 (72) for a phenyl substituent]. Not only are changes in electron delocalization expected to enhance catalysis but the 2-naphthylglycolate enolic intermediate should also be stabilized by the putative cation– π interaction similar to mandelate as discussed above. Consequently, one would expect the point corresponding to 2-naphthohydroxamate in Figure 3B to lie below the regression line, similar to benzohydroxamate. However, this is not the case. Although 2-naphthylglycolate and mandelate are bound with similar affinity in the ground state ($\Delta\Delta G_{2\text{-naphthylglycolate-mandelate}} \approx 0.3$ kcal/mol), they exhibit a larger difference between their transition state stabilization free energies ($\Delta\Delta G_{2\text{-naphthylglycolate-mandelate}} \approx -1.4$ kcal/mol). Thus racemization of the bulkier 2-naphthylglycolate is sensitive to steric constraints in the enzyme–intermediate complex, and it follows from the Hammond postulate (74) that the binding affinity of the 2-naphthohydroxamate intermediate analogue should be reduced relative to benzohydroxamate. Our observation that the binding free energy for 2-naphthohydroxamate is 0.9 kcal/mol less favorable than the free energy for binding benzohydroxamate is in accord with this expectation.

CONCLUSIONS

In general, the free energy changes accompanying binding of MR with both substrate and intermediate analogues bearing alkyl groups in place of the phenyl group are proportional to the corresponding hydrophobicity of the group (π) and the VDW surface areas of the ligands. The VDW surface area dependence of the free energy change accompanying desolvation of the hydrophobic surface during intermediate analogue binding (-41 ± 3 cal mol⁻¹ Å⁻²) is about 10 cal mol⁻¹ Å⁻² greater than that observed for ground state binding (-30 ± 5 cal mol⁻¹ Å⁻²). Interestingly, the intermediate analogue benzohydroxamate is bound 2 orders of magnitude more tightly than would be predicted on the basis of correlations with π values or the VDW surface areas. This suggests that specific polar interactions with the phenyl group stabilize the mandelate enolic intermediate relative to the ground state. MR exhibited reduced stabilization of 2-naphthylglycolate in the transition state (relative to mandelate in the transition state) and reduced binding of

2-naphthohydroxamate relative to benzohydroxamate. These observations indicate that steric constraints within the hydrophobic cavity of the MR–intermediate complex are more stringent than those in the MR–substrate complex.

REFERENCES

- Hegeman, G. D., Rosenberg, E. Y., and Kenyon, G. L. (1970) *Biochemistry* 9, 4029–4036.
- Kenyon, G. L., Gerlt, J. A., Petsko, G. A., and Kozarich, J. W. (1995) *Acc. Chem. Res.* 28, 178–186.
- Kenyon, G. L., and Hegeman, G. D. (1979) *Adv. Enzymol. Relat. Areas Mol. Biol.* 50, 325–360.
- Powers, V. M., Koo, C. W., Kenyon, G. L., Gerlt, J. A., and Kozarich, J. W. (1991) *Biochemistry* 30, 9255–9263.
- Kallarakal, A. T., Mitra, B., Kozarich, J. W., Gerlt, J. A., Clifton, J. G., Petsko, G. A., and Kenyon, G. L. (1995) *Biochemistry* 34, 2788–2797.
- Landro, J. A., Gerlt, J. A., Kozarich, J. W., Koo, C. W., Shah, V. J., Kenyon, G. L., Neidhart, D. J., Fujita, S., and Petsko, G. A. (1994) *Biochemistry* 33, 635–643.
- Mitra, B., Kallarakal, A. T., Kozarich, J. W., Gerlt, J. A., Clifton, J. G., Petsko, G. A., and Kenyon, G. L. (1995) *Biochemistry* 34, 2777–2787.
- St. Maurice, M., and Bearne, S. L. (2000) *Biochemistry* 39, 13324–13335.
- Chiang, Y., Kresge, A. J., Pruszyński, P., Schepp, N. P., and Wirz, J. (1990) *Angew. Chem., Int. Ed. Engl.* 29, 792–794.
- Gerlt, J. A., and Gassman, P. G. (1993) *Biochemistry* 32, 11943–11952.
- Gerlt, J. A., and Gassman, P. G. (1993) *J. Am. Chem. Soc.* 115, 11552–11568.
- Babbitt, P. C., and Gerlt, J. A. (1997) *J. Biol. Chem.* 272, 30591–30594.
- Babbitt, P. C., Hasson, M. S., Wedekind, J. E., Palmer, D. R., Barrett, W. C., Reed, G. H., Rayment, I., Ringe, D., Kenyon, G. L., and Gerlt, J. A. (1996) *Biochemistry* 35, 16489–16501.
- Gerlt, J. A. (1998) in *Bioorganic Chemistry: Peptides and Proteins* (Hecht, S. M., Ed.) pp 279–311, Oxford University Press, New York.
- Gerlt, J. A., Kenyon, G. L., Kozarich, J. W., Neidhart, D. C., and Petsko, G. A. (1992) *Curr. Opin. Struct. Biol.* 2, 736–742.
- Schafer, S. L., Barrett, W. C., Kallarakal, A. T., Mitra, B., Kozarich, J. W., Gerlt, J. A., Clifton, J. G., Petsko, G. A., and Kenyon, G. L. (1996) *Biochemistry* 35, 5662–5669.
- Neidhart, D. J., Howell, P. L., Petsko, G. A., Powers, V. M., Li, R. S., Kenyon, G. L., and Gerlt, J. A. (1991) *Biochemistry* 30, 9264–9273.
- Felfer, U., Strauss, U. T., Kroutil, W., Fabian, W. M. F., and Faber, K. (2001) *J. Mol. Catal. B: Enzym.* 15, 213–222.
- Kenyon, G. L., and Hegeman, G. D. (1970) *Biochemistry* 9, 4036–4043.
- St. Maurice, M., and Bearne, S. L. (2002) *Biochemistry* 41, 4048–4058.
- Lin, D. T., Powers, V. M., Reynolds, L. J., Whitman, C. P., Kozarich, J. W., and Kenyon, G. L. (1988) *J. Am. Chem. Soc.* 110, 323–324.
- Landro, J. A., Kenyon, G. L., and Kozarich, J. W. (1992) *Bioorg. Med. Chem. Lett.* 2, 1411–1418.
- Li, R., Powers, V. M., Kozarich, J. W., and Kenyon, G. L. (1995) *J. Org. Chem.* 60, 3347–3351.
- Bearne, S. L., and Wolfenden, R. (1997) *Biochemistry* 36, 1646–1656.
- Mader, M. M., and Bartlett, P. A. (1997) *Chem. Rev.* 97, 1281–1301.
- Radzicka, A., and Wolfenden, R. (1995) *Methods Enzymol.* 249, 284–312.
- Wolfenden, R., and Frick, L. (1987) in *Enzyme Mechanisms* (Page, M. I., and Williams, A., Eds.) pp 97–122, Royal Society of Chemistry, London.
- Wolfenden, R., Snider, M. J., Ridgway, C., and Miller, B. (1999) *J. Am. Chem. Soc.* 121, 7419–7420.
- Landro, J. A., Kallarakal, A. T., Ransom, S. C., Gerlt, J. A., Kozarich, J. W., Neidhart, D. J., and Kenyon, G. L. (1991) *Biochemistry* 30, 9274–9281.
- Guthrie, J. P., and Kluger, R. (1993) *J. Am. Chem. Soc.* 115, 11569–11572.

31. Bearne, S. L., St. Maurice, M., and Vaughan, M. D. (1999) *Anal. Biochem.* 269, 332–336.
32. Maggio, E. T., Kenyon, G. L., Mildvan, A. S., and Hegeman, G. D. (1975) *Biochemistry* 14, 1131–1139.
33. Compere, J. E. L. (1968) *J. Org. Chem.* 33, 2565–2566.
34. Kinbara, K., Harada, Y., and Saigo, K. (2000) *J. Chem. Soc., Perkin Trans. 2*, 1339–1347.
35. Howe, R., Moore, R. H., and Rao, B. S. (1973) *J. Med. Chem.* 16, 1020–1023.
36. Summers, J. B., Mazdiyasni, H., Holms, J. H., Ratajczyk, J. D., Dyer, R. D., and Carter, G. W. (1987) *J. Med. Chem.* 30, 574–580.
37. Pirrung, M. C., and Chau, J. H.-L. (1995) *J. Org. Chem.* 60, 8084–8085.
38. Nagarajan, K., Rajappa, S., Rajagopalan, P., and Talwalkar, P. K. (1991) *Indian J. Chem.* 30B, 222–229.
39. Larsen, K., Sjöberg, B.-M., and Thelander, L. (1982) *Eur. J. Biochem.* 125, 75–81.
40. Johnson, J. E., Ghafouripour, A., Haug, Y. K., Cordes, A. W., Pennington, W. T., and Exner, O. (1985) *J. Org. Chem.* 50, 993–997.
41. Berndt, D. C., and Shechter, H. (1964) *J. Org. Chem.* 29, 916–918.
42. Fishbein, W. N., Daly, J., and Streeter, C. L. (1969) *Anal. Biochem.* 28, 13–24.
43. Sosnovsky, L., and Krogh, L. (1980) *Synthesis*, 654–656.
44. Sharp, T. R., Hegeman, G. D., and Kenyon, G. L. (1979) *Anal. Biochem.* 94, 329–334.
45. Sjöberg, P., and Politzer, P. (1990) *J. Phys. Chem.* 94, 3959–3961.
46. Fersht, A. (1999) *Structure and Mechanism in Protein Science*, W. H. Freeman, New York.
47. Fee, J. A., Hegeman, G. D., and Kenyon, G. L. (1974) *Biochemistry* 13, 2528–2532.
48. Burley, S. K., and Petsko, G. A. (1988) *Adv. Protein Chem.* 39, 125–189.
49. Dougherty, D. A. (1996) *Science* 271, 163–168.
50. Chilov, G. G., Guranda, D. T., and Svedas, V. K. (2000) *Biochemistry (Moscow)* 65, 1135–1139.
51. Fastrez, J., and Fersht, A. R. (1973) *Biochemistry* 12, 1067–1074.
52. Fierke, C. A., Calderone, T. L., and Krebs, J. F. (1991) *Biochemistry* 30, 11054–11063.
53. Krebs, J. F., Rana, F., Dluhy, R. A., and Fierke, C. A. (1993) *Biochemistry* 32, 4496–4505.
54. Nair, H. K., Seravalli, J., Arbuckle, T., and Quinn, D. M. (1994) *Biochemistry* 33, 8566–8576.
55. Shibaev, V. N., Eliseeva, G. I., and Kochetkov, N. K. (1975) *Biochim. Biophys. Acta* 403, 9–16.
56. Hansch, C., and Leo, A. (1979) *Substituent Constants for Correlation Analysis in Chemistry and Biology*, John Wiley & Sons, New York.
57. St. Maurice, M., Bearne, S. L., Lu, W., and Taylor, S. D. (2003) *Bioorg. Med. Chem. Lett.* 13, 2041–2044.
58. Burkhard, P., Taylor, P., and Walkinshaw, M. D. (2000) *J. Mol. Biol.* 295, 953–962.
59. Eriksson, A. E., Baase, W. A., Zhang, X.-J., Heinz, D. W., Blaber, M., Baldwin, E. P., and Matthews, B. W. (1992) *Nature* 255, 178–183.
60. Sharp, K. A., Nicholls, A., Friedman, R., and Honig, B. (1991) *Biochemistry* 30, 9686–9697.
61. Chothia, C. (1975) *Nature* 254, 304–308.
62. Farkas, E., Enyedy, E. A., and Csoka, H. (2000) *J. Inorg. Biochem.* 79, 205–211.
63. Lins, L., Thomas, A., and Brasseur, R. (2003) *Protein Sci.* 12, 1406–1417.
64. Breslow, E., Mombouyran, V., Deeb, R., Zheng, C., Rose, J. P., Wang, B. C., and Haschemeyer, R. H. (1999) *Protein Sci.* 8, 820–831.
65. Hiratake, J., Irie, T., Tokutake, N., and Oda, J. (2002) *Biosci., Biotechnol., Biochem.* 66, 1500–1514.
66. Ma, J. C., and Dougherty, D. A. (1997) *Chem. Rev.* 97, 1303–1324.
67. Perutz, M. F. (1993) *Philos. Trans. R. Soc. London, Ser. A* 345, 105–112.
68. Fernández-Recio, J., Romero, A., and Sancho, J. (1999) *J. Mol. Biol.* 290, 319–330.
69. Fernández-Recio, J., Vázquez, A., Civera, C., Sevilla, P., and Sancho, J. (1997) *J. Mol. Biol.* 267, 184–197.
70. Loewenthal, R., Sancho, J., and Fersht, A. R. (1992) *J. Mol. Biol.* 224, 759–770.
71. Golas, C. L., Prokipcak, R. D., Okey, A. B., Manchester, D. K., Safe, S., and Fujita, T. (1990) *Biochem. Pharmacol.* 40, 737–741.
72. Brown, H. C., and Okamoto, Y. (1958) *J. Am. Chem. Soc.* 80, 4979–4987.
73. van Leuwen, B. G., and Ouellette, R. J. (1968) *J. Am. Chem. Soc.* 95, 7056–7060.
74. Hammond, G. S. (1955) *J. Am. Chem. Soc.* 77, 334–338.
75. Leo, A., Hansch, C., and Elkins, D. (1971) *Chem. Rev.* 71, 525–616.
76. Leo, A., Jow, P. Y. C., Silipo, C., and Hansch, C. (1975) *J. Med. Chem.* 18, 865–868.

BI036207X